Desalination and Water Treatment
www.deswater.com
doi: 10.5004/dwt.2019.24669

169 (2019) 353–362
November

Sorption of acidic dyes from water by poly(vinyl imidazole) grafted onto poly(styrene) based beads

Fatih Bildik[a], Gülçin Torunoglu Turan[a], Hakan Duran[b], Tuba Şişmanoğlu[b], Bahire Filiz Senkal[a,*]

[a]*Department of Chemistry, Istanbul Technical University, Maslak 34469 Istanbul, Turkey, emails: bsenkal@itu.edu.tr (B.F. Senkal), bildikfatih@itu.edu.tr (F. Bildik), torunoglugulcin@gmail.com (G.T. Turan)*
[b]*Engineering Faculty, Department of Chemistry, Istanbul University-Cerrahpasa, 34850 Istanbul, Turkey, emails: tusase3@gmail.com (H. Duran), tusase@istanbul.edu.tr (T. Şişmanoğlu)*

Received 28 January 2019; Accepted 2 July 2019

ABSTRACT

In the first stage of this study, poly (vinyl benzyl chloride-co-ethylene glycol dimethacrylate [EGDMA]) (10%) (PVBC) resin was prepared by suspension polymerization method using toluene as porogen, poly(vinyl alcohol) as stabilizator and AIBN as initiator. Then, poly (vinyl imidazole) (PVI) was grafted on the PVBC resin with a particle size of 200–400 μm through the 2-chloromethyl group to obtain core-shell type resin by using reverse atom transfer radical polymerization (ATRP) method. Grafting degree reached to about 57% and the PVI-grafted resin has been shown to be effectively used to remove dye even at ppm levels. The adsorption behavior of the PVI-grafted resin was investigated using Freundlich, Langmuir, Flory–Huggins and Dubinin–Radushkevich isotherms models. To observe trace dye sorption characteristic of the resin, kinetic models were applied.

Keywords: ATRP; Grafting; Poly (vinyl imidazole); Dye sorption; Polymeric resin

1. Introduction

Toxicity and carcinogenicity of many dyes seriously affect the aquatic living organisms. Due to the fact that dyes are persistent organic molecules, resistant to aerobic assimilation, and are firm to light, heat, and oxidizing agents, treatment of the dye-containing wastewater is difficult. Several chemical, physical and biological decolorization methods have been utilized. Surface modification has been of importance to offer polymers with desired properties for practical applications [1].

Grafting linear polymers onto crosslinked resins combines the solubility and flexibility of the graft polymer side chains as the functional group carrier and this presents various potential applications. Two common techniques so called 'grafting from' and 'grafting onto' have limited success in most cases [2].

'Grafting from' by radical initiation is the most prevalent method which involves the use of anchored initiation sites on the solid surface. The flexible side-chains can provide pseudo-homogeneous reaction conditions and better accessibility of the involved functional groups. This method suffers from the formation of significant amounts of homopolymer as a side reaction due to radical fragments detached from the surface. Different approaches [3,4] including radiation induced grafting via hydroperoxy groups on solid polymers [5] have been reported to overwhelm homopolymer formation.

* Corresponding author.

One of the important methods uses polymer-supported chain transfer agents in combination with a common azo initiator as a radical source [6].

Amongst the surface functionalization methods, surface initiated atom transfer radical polymerization (SI-ATRP) technique has attracted interest for the surface grafting high-density polymer brushes with controlled molecular weight, molecular weight distribution and well-defined structure [2,7–9]. Furthermore, ATRP can be initiated on surfaces of synthetic and natural polymers for several purposes. This technique can be used even in heterogeneous conditions successfully and grafting from solid particles can be obtained with reasonable polydispersities. Additionally, almost all the polymers formed were chemical bonded onto the matrices and no free polymers were obtained in the SI-ATRP procedures [10–12].

More importantly, ATRP provides a relatively easy pathway to core-shell type of polymers. Commercial halogenated polyolefins, such as poly (vinyl chloride) (PVC), poly (vinylidene fluoride) (PVDF), poly (chlorotrifluoroethylene) (PCTFE), and their copolymers are potential ATRP macro initiators [13,14].

Modified silicone surfaces have also been used to graft acrylamide monomers by metal-mediated ATRP [15]. Bromo t-butyl ester of Wang resin was used as initiator in copper-mediated ATRP for grafting methyl methacrylate (MMA) and copolymer blocks [16]. Several acrylate polymers have been grafted from chloromethyl groups on crosslinked polystyrene beads [17]. Polymer supported N-chloro sulfonamide polymer was used as ATRP macro initiator for grafting acrylates [18] and acrylamide [19].

Poly (vinyl pyrrolidone) was grafted onto styrene-based resin by ATRP method in our previous work [20]. This method was also used to graft poly(1-ethyl-3-(2-methacryloyloxy ethyl) imidazolium chloride) brushes onto gold surfaces [21].

In this study, this analogy has been extended to chloromethyl group to prepare poly (vinyl imidazole) graft chains on crosslinked PVBC.

Imidazole ring can be utilized as a bio agent revolving around its ability to bond to metals as a ligand [22–26] and to form hydrogen bond with drugs and proteins. Also, it is resistant to hydrogenation and high chemical stability against harsh acids and bases [27].

It is well known that there is a high affinity between amine groups and acid dyes. Therefore, the new resulting PVI grafted resin was shown to efficiently remove Calcon, Remazol black B and Reactive red 195 as acidic dyes from water.

2. Materials and methods

2.1. Materials

All chemicals used were of analytical grade: vinyl benzyl chloride (VBC) (Sigma-Aldrich, Netherlands), ethyleneglycol dimethacrylate (EGDMA) (Sigma-Aldrich), vinyl imidazole (Sigma-Aldrich), remazol Black B (Sigma-Aldrich), Calcon (Sigma-Aldrich), Reactive Red 195 (Sigma-Aldrich), N,N,N′, N″,N″-Pentamethyldiethylenetriamine (PMDETA, England) (Fluka), CuBr (Sigma-Aldrich) and $CuBr_2$ (Sigma-Aldrich). All chemicals were analytical grade and were used without further purification.

2.2. Preparation of the crosslinked PVBC resin

The crosslinked PVBC-co-EGDMA (10% mol) resin was prepared according to previously reported procedures [28].

2.3. Grafting 'from' resin

Graft polymerization of vinyl imidazole was achieved through 2-chloroethyl functional group initiation sites on the PVBC resin.

A typical procedure is as follows:

0.144 g (0.01 mol) CuBr, 0.0672 g (0.30 mmol) $CuBr_2$, 0.62 mL (4.31 mmol) of the PMDETA ligand and 10 mL (0.110 mol) vinyl imidazole were successively put in a three-necked flask equipped with a reflux condenser and nitrogen inlet. Crosslinked PVBC resin sample (2.0 g) was added to the flask under nitrogen atmosphere and the graft polymerization was proceeded at 130°C for 72 h. The reaction content was poured into 100 mL of distilled water at the end of the grafting reaction. The obtained PVI grafted resin was filtered and interacted with 5.0% of EDTA solution to remove copper salts. Then, the resin was filtered and washed with excess of water (300 mL) and alcohol (20 mL) to remove soluble contaminants. The PVI grafted resin was dried under vacuum for 24 h at room temperature. Dried sample weighed 3.186 g.

The grafting percentage was determined from the mass of dried resin before and after grafting as follows:

$$\text{Percentage grafting} = \left[\frac{(W_2 - W_1)}{W_1}\right] \times 100 \quad (1)$$

where W_1 and W_2 are the masses of the PVBC and PVI grafted resins, respectively.

2.4. Determination of amine content of the resin

For this purpose, 0.10 g of the resin sample was interacted with 20 mL of HCl (0.10 M) solution for 10 h at room temperature. After separation of the resin from the solution by centrifugation, 2.0 mL of non-interacted acidic solution sample was titrated with 0.050 M NaOH solution and phenolphathalein was used as an indicator. The quantity of the total amine content of the resin was calculated as 4.50 mmol per g of the resin.

2.5. Determination of the optimum amount of the sorbent

The optimum resin quantity experiments were examined as follows: between 0.050 and 0.25 g of the resin samples were wetted with 1 mL of distilled water. After that, resins were mixed with 10 mL of dye solution (1.0 g dye/50 mL water) and stirred for 24 h at room temperature. Then, the mixture was centrifugated and dye sorption capacities were measured colorimetrically described below.

2.6. Extraction of dyes

The adsorption of reactive dyes on the resin was performed in a batch system. Calcon, Remazol Black B and Reactive Red 195 as acidic dyes were in these experiments.

Dye sorption capacities of the resin was determined by mixing weighed amount of resin sample (0.20 g) with 10 mL of different initial dye concentrations (1.00 g–0.555 dye g/50 mL water). The mixtures were stirred at room temperature for 24 h and after centrifugation, the amounts of un-adsorbed dyes in supernatant solutions were analyzed colorimetrically using a UV–Vis spectrophotometer at their respective absorbance maxima.

2.7. Dye sorption kinetics

In order to estimate the efficiency of the resin, experiments of batch kinetics were carried out using highly diluted dye solutions (0.80 mg dye/mL water). For this purpose, the resin (0.10 g) was wetted with distilled water (1.50 mL) and added to a solution of dye (100 mL). The mixtures were stirred with a magnetic stirring bar and 5.0 mL of samples from the solution were taken at appropriate time intervals to determine the non-adsorbed dye contents by the method as described above.

2.8. Regeneration of the resin

Desorption experiments were carried out using dye-interacting resins for 24 h. Before subjecting to the desorption experiment, dye-loaded resin was separated from the solution by centrifuge, washed with distilled water several times, and finally dried under a vacuum. Then, the dye-loaded sample (0.20 g) was mixed with 50 mL 10% KOH in methanol solution and was refluxed for 6 h. Then, the solution was cooled and the resin was separated by centrifuge, and the dye-containing solution was diluted with water properly and neutralized with HCl solution.

3. Results and discussion

In this study, poly (PVBC-co-EGDMA) resin was prepared by suspension polymerization method. The resin was sieved, and the 200–400 μm size fractions were used in the experiments.

Core-shell type of polymer with PVI shells were obtained by reverse ATRP method. Graft polymerization of vinyl imidazole was obtained from 2-chloroethyl groups on PVBC resin (Fig. 1).

Although polymerization is heterogeneous in nature, it proceeds with progressive mass increase at 130°C. The grafting degree reaches to about 57% for 72 h. The resins were characterized using FT-IR spectra.

According to Fig. 2, PVBC resin showed a characteristic C–Cl stretching at about 671 cm^{-1}. In the resin, asymmetric stretching of methyl and methylene groups was observed at 2,919 cm^{-1}, respectively. Symmetric stretching peak of methylene group was found at 2,835 cm^{-1} and the bands at 1,589 and 1,449 cm^{-1} belong to CN symmetric stretching vibrations in the imidazole ring respectively. Also, C–N stretching mode of ring occurs at 812 and 689 cm^{-1}.

Morphological characterizations of the resins were investigated by SEM. After grafting with PVI, the pores of the PVBC resin seem to be filled with grafted polymer and the surface of the PVI grafted resin is smoother than that of the plain resin (Fig. 3b). It can also be seen in the SEM images

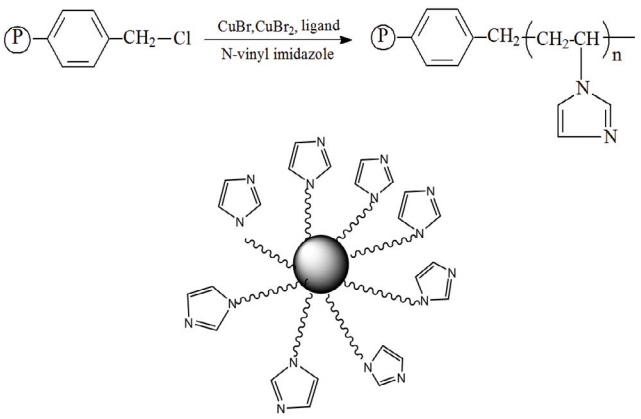

Fig. 1. Preparation of the core-shell type resin.

that the shapes of the grafted resin (Fig. 3b) cracked, because of heating and stirring during polymerization.

3.1. Extraction of dyes

Batch experiments of dye sorption were performed at room temperature by depending on different initial dye concentrations. Residual dye contents were determined by colorimetrical analysis and dye sorption capacities were calculated by the difference from non-adsorbed and adsorbed dye concentrations. In this study, dye sorption of the resin was studied by FTIR spectroscopy. After interaction of resin with dyes (Remazol black B) in Fig. 2, –N=N– stretching and C–C stretching frequencies of azo groups and aromatic rings were observed at 1,593; 1,488; 1,421 cm^{-1}, respectively. On the other hand, the peaks at 1,338 and 1,280.73 cm^{-1} indicated C–N stretching frequencies of aromatic carbons attached with nitrogen functionality. The peaks at 1,125 and 659 cm^{-1} represented S=O stretching frequency of SO_3 Na group on aromatic ring. Also, PVI grafted resin original peaks shifted after dye sorption. According to the FTIR results, PVI grafted resin was interacted with dyes.

In aqueous solutions, the reactive dye was dissolved and the sulfonate group of the reactive dye was dissociated and converted to anionic dye ions [29]:

$$DyeSO_3Na + H_2O \rightarrow DyeSO_3^- + Na^+ \quad (1)$$

The unpaired electrons of PVI brushes of the resin will have a positive charge (Fig. 4), because of hybridization of the nitrogen atom, capable of forming the salt with the anionic groups of the acid dye molecules [30].

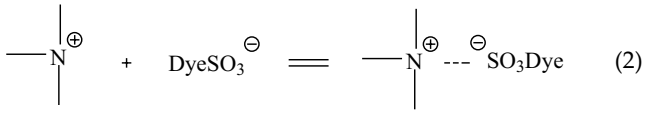

(2)

3.2. Adsorption isotherms

All the sorption experiments were conducted at 25°C. The percentage of uptake of acidic dyes and amount adsorbed (mol g^{-1}) were calculated by using the following relationships:

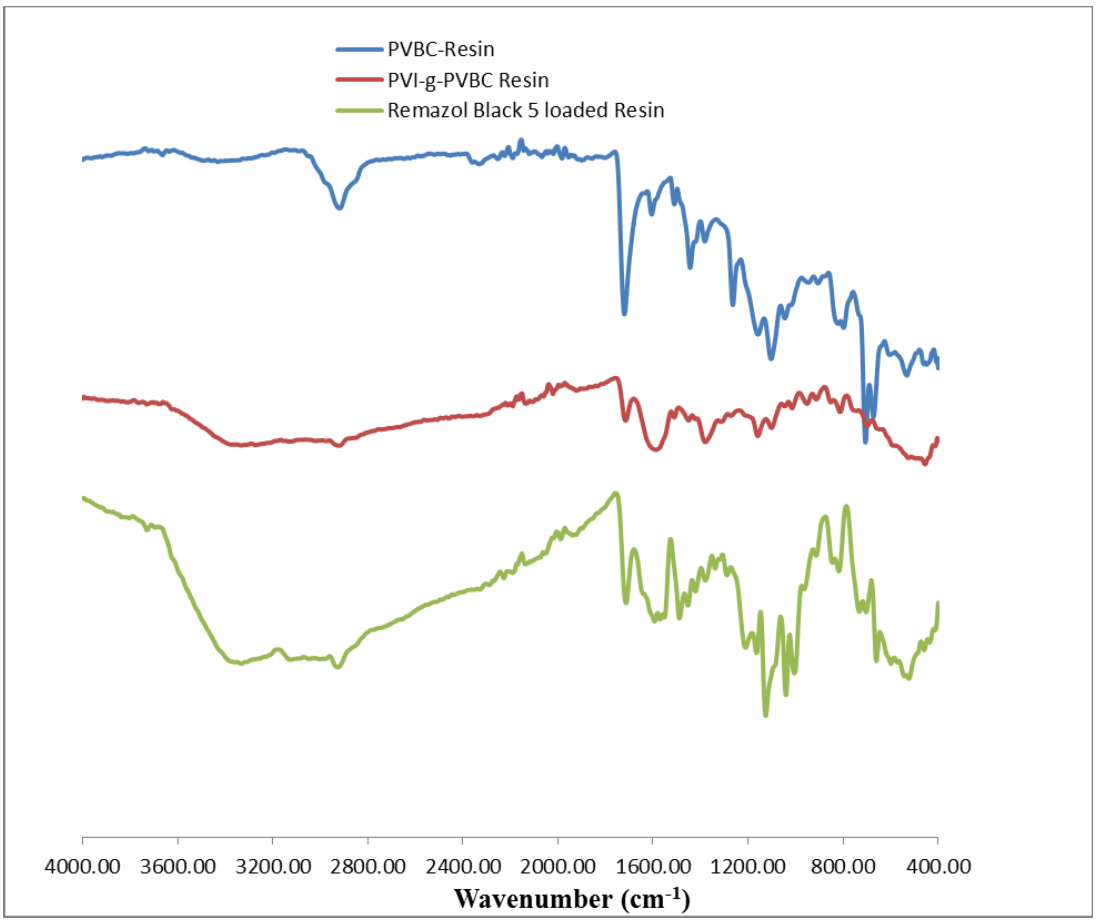

Fig. 2. FTIR spectra of the resins.

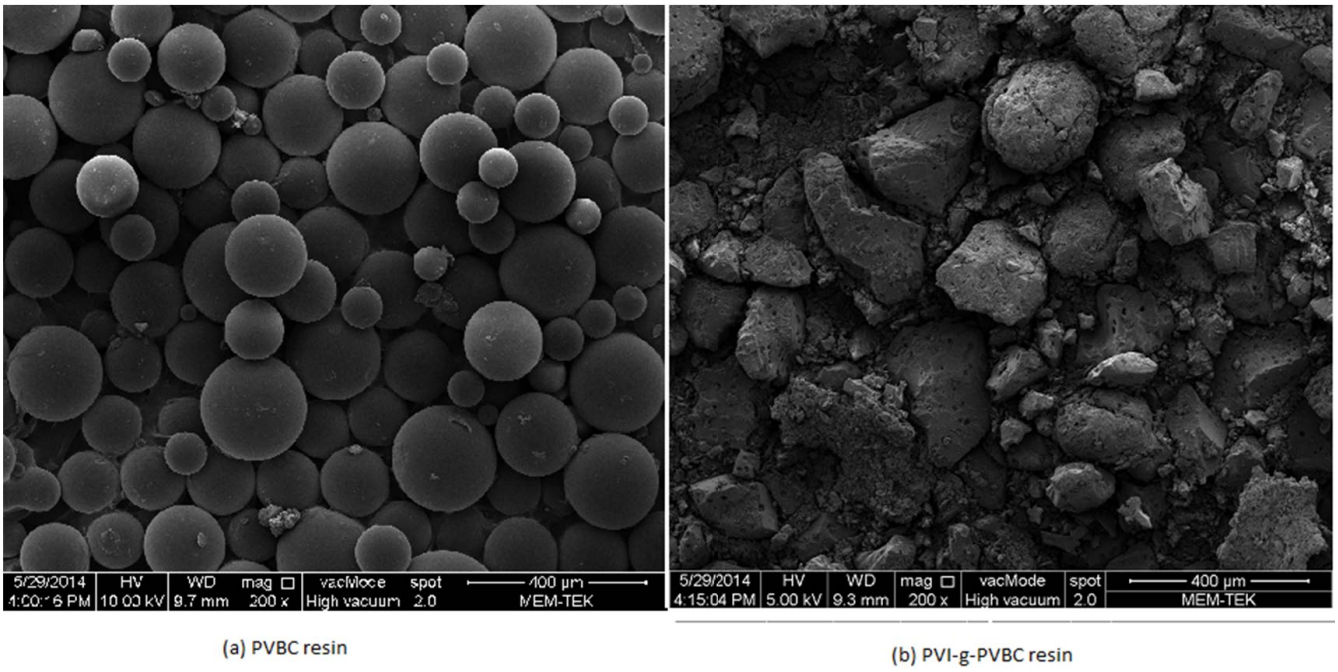

Fig. 3. SEM image of the (a) PVBC resin and (b) PVI grafted resin.

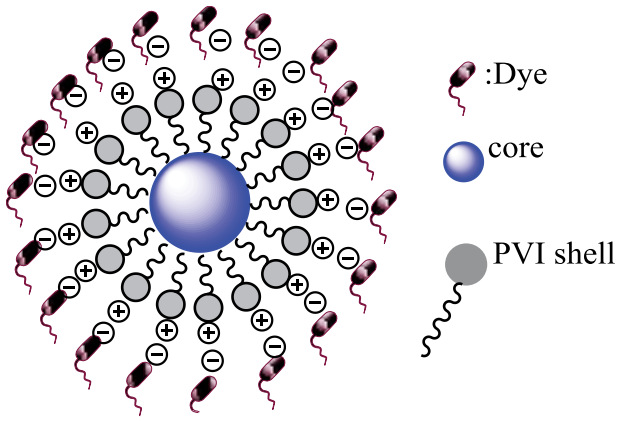

Fig. 4. Dye–polymer interaction.

$$\text{dye uptake } \% = 100\frac{(C - C_t)}{C} \tag{4}$$

$$q_e = V\frac{(C - C_t)}{m} \tag{5}$$

where q_e is the amount adsorbed, C and C_t are the initial concentration and the concentration (mol L^{-1}) at time t, respectively, and m is the mass of resin (g) and V (L) is the volume of solution.

Isotherm type of this adsorption process is similar to Giles isotherms L type as seen in Fig. 5. For Reactive Red 195, Remazol Black B and Calcon, the first curvature shows that as more sites in the adsorbent are filled, it becomes increasingly difficult for adsorbate to find a blank site available. This implies that the adsorbate is flat-oriented. Substances that have very strong intermolecular attractions are adsorbed from water by ion–ion attraction. It is possible that the adsorbed dyes may have turned into joint into very large stack before adsorption took place.

3.2.1. Freundlich isotherm

The Freundlich isotherm model can be applied by the following equation for multi-layer adsorption on heterogeneous surfaces.

$$q_e = K_F C_e^n \tag{6}$$

The linear equation of the Freundlich isotherm is fitted as the logarithmic form as given below:

$$\log q_e = \log K_F + n \log C_e \tag{7}$$

where q_e is amount adsorbed (mg g^{-1}), C_e is the equilibrium concentration in aqueous phase (mg L^{-1}), K_F is adsorption capacity and n is adsorption intensity. When $\log q_e$ is plotted against $\log C_e$ with slope n and intercept $\log K_F$ is obtained as seen in Fig. 6a and Freundlich constants are given in Table 1.

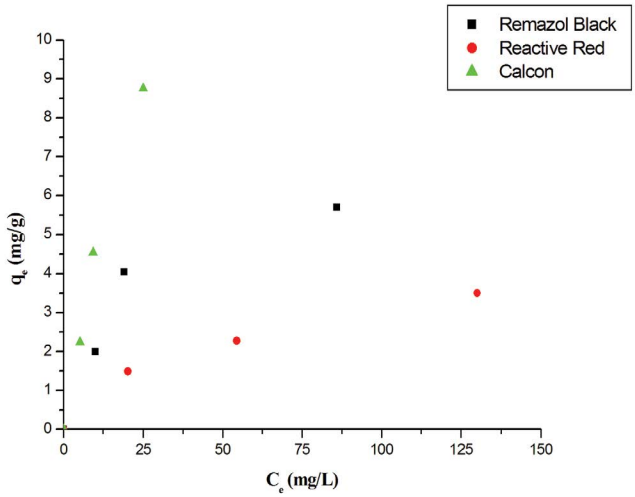

Fig. 5. Isotherm types.

Table 1
Isotherm parameters, value of the Gibbs free energy G and value of the bonding free energy E

Isotherms	Calcon	Remazol Black B	Reactive Red 195
	Freundlich		
N	0.850	0.46	0.44
K_F	0.600	0.75	1.74
R^2	0.970	100	83.1
	Langmuir		
q_{max} mg g^{-1}	111	4.11	9.70
K_L L mg^{-1}	4×10^{-3}	2.8×10^{-2}	2.7×10^{-2}
R^2	0.982	98.4	94.0
	D-R		
q_{max} mg g^{-1}	8.50	3.05	5.65
K_{DR}	7.40	51.2	18.8
E/J mol^{-1}	261	99.0	163
R^2	0.960	84.0	100
	F-H		
K_{FH}	3.1×10^{-10}	3.5×10^{-4}	7.1×10^{-4}
DG/kJ mol^{-1} K^{-1}	54	20	18
R^2	0.990	98.0	95.0

3.2.2. Langmuir isotherm

Langmuir's isotherm model is effective for monolayer adsorption onto a surface containing a limited number of similar sites. The equation of the most widely applied model is represented as follows:

$$\frac{1}{q_e} = \frac{1}{q_{max}} + \frac{1}{q_{max} b C_e} \tag{8}$$

where q_{max} is the maximum adsorption at monolayer coverage (mg g^{-1}) and b is the adsorption equilibrium constant

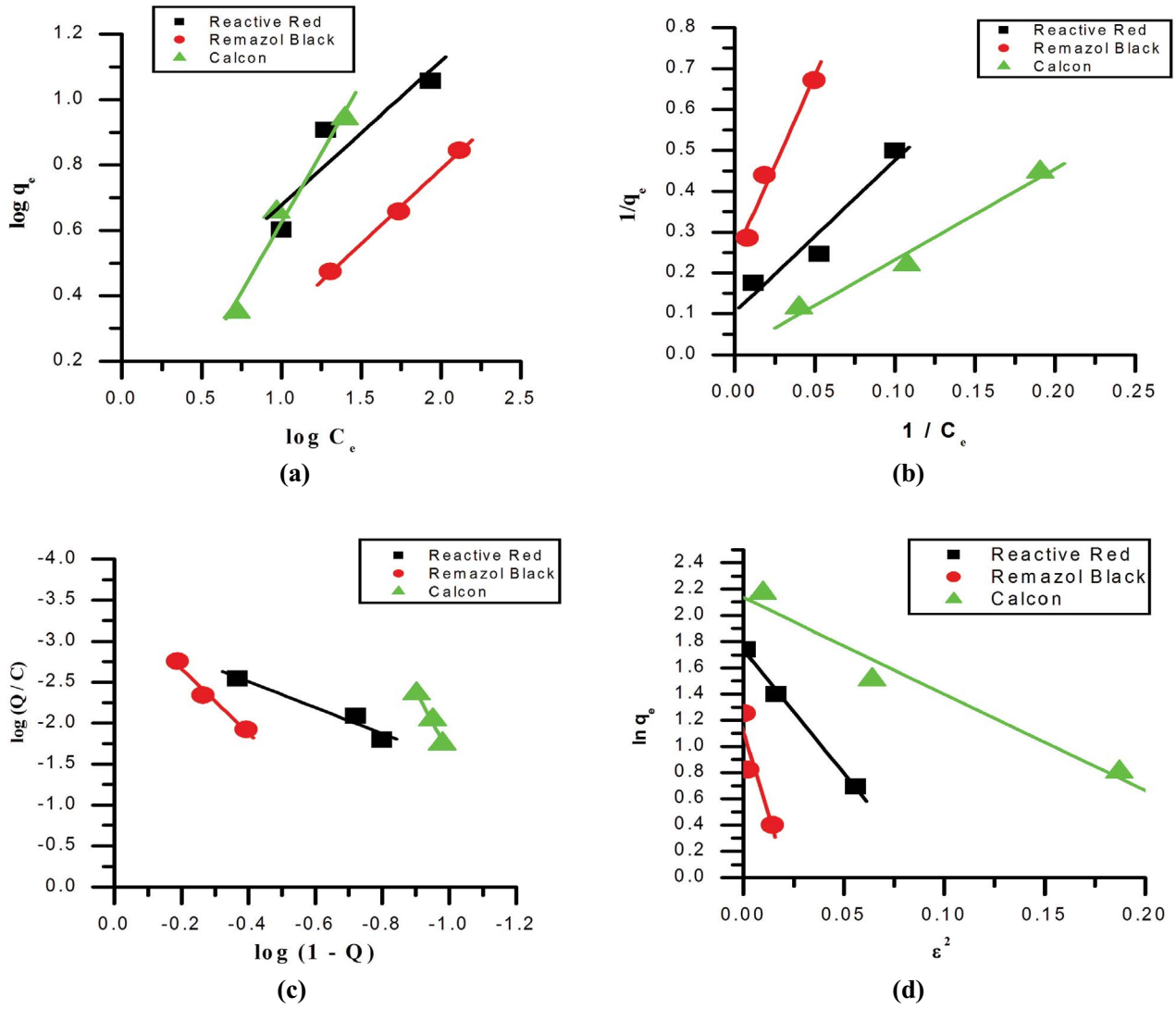

Fig. 6. Adsorption isotherm models of the resin: (a) Freundlich, (b) Langmuir, (c) Flory–Huggins, (d) Dubinin–Radushkevich.

(L mg^{-1}). $1/q_e$ vs. $1/C_e$ with slope b and intercept $1/q_{max}$ is obtained as seen in Fig. 6b. This graph indicates that the adsorption fit Langmuir isotherm model for resin as seen in Fig. 6b.

The maximum adsorption values of the adsorbent have been found as 111, 9.70 and 4.11 mg g^{-1} for Calcon, Reactive Red 195 and Remazol Black B, respectively, as given in Table 1.

3.2.3. Flory–Huggins isotherm (F-H)

The F-H model was generally used to account for the degree of surface coverage characteristics of the adsorbate on the adsorbent. The linear form of the F-H equation is represented as follows:

$$\log\frac{Q}{C} = \log K_{FH} + n\log\left(1-Q\right) \tag{9}$$

where $Q = (1 - C_e/C)$ is the degree of surface coverage, n is the number of adsorbates occupying adsorption sites, K_{FH} is the equilibrium constant. n and K_{FH} values are obtained from the slope and intercept of the curve log Q/C vs. log (1–Q) drawn as seen in Fig. 6c.

The Gibbs free energy is related to equilibrium constant as follows [31]:

$$\Delta G = -\,2.303\,RT\log K_{FH} \tag{10}$$

where T is temperature (K), R is gas constant, 8.314 J mol^{-1} K^{-1}. The F-H parameters, n and K_{FH}, are given Table 1. $\Delta G > 0$ indicate that the adsorption process is non-spontaneous in nature and supports an endothermic reaction as seen in Table 1. The Gibbs free energy values of the resin were found as 54, 20 and 18 kJ mol^{-1} respectively.

3.2.4. Dubinin–Radushkevich isotherm (D-R)

D-R isotherm is suitable for describing the mechanism of adsorption to a heterogeneous surface by the Gauss energy

distribution. Here, q_e is the amount of adsorbate in the adsorbent at equilibrium (mg g^{-1}). q_{max}, saturation capacity (mg g^{-1}) and Dubinin–Radushkevich isotherm constant (e) was calculated as seen in Eq. (11). K_{DR} Dubinin–Radushkevich isotherm constant (mol^2 kJ^{-2}) was used for calculating bonding free energy as seen in Eq. (12). q_{max} and K_{DR} values are obtained from the slope and intercept of the curve e^2 vs. ln q_e drawn as seen in Fig. 6d. The equation is convenient to separate the physical and chemical adsorption uptake of dyes on polymeric adsorbent.

$$\ln q_e = \ln q_{max} - K_{DR}e^2 \tag{11}$$

$$e = RT \ln\left(1+\frac{1}{C_e}\right) \quad E = \frac{1}{\sqrt{2K_{DR}}} \tag{12}$$

The bonding free energies of dyes on the resin were found to be 261, 163 and 99 J mol^{-1} for Calcon, Reactive Red 195 and Remazol Black B, respectively, by using D-R isotherm. These values shown in Table 1 indicate the adsorption process to be a physisorption.

3.2.5. Effect of resin quantity on dye sorption

Different amount of resins were used to determine optimum sorbent quantity. For this purpose, 0.025–0.25 g of resins were interacted with 10 mL of dye solution (0.555 dye g/50 mL) water for 24 h at room temperature. In this experiment, Calcon was used as acidic dye. Non-adsorbed dye concentrations were determined colorimetrically. All results were given in Table 2. According to the results, sorption capacity of dye increases until 0.20 g of the resin. The highest sorbent value was found as 0.20 g. This value was used for other experiments.

pH-dependent experiments were also carried out in this study. The interaction between sorbate and sorbent is affected by the pH of an aqueous medium in two ways: first, since dyes are complex aromatic organic compounds having different functional groups and unsaturated bonds, they have different ionization potentials at different pH, resulting in the pH dependent net charge on dye molecules. Second, the surface of the resin includes many functional groups, so the net charge on sorbent is also pH dependent.

Therefore, the interaction between dye molecules and sorbent resin are basically a combined result of charges on dye molecules and the surface of sorbent.

The PVI grafted PVBC resin can be used in lower pH values and a wide pH range (Table 3). Under acidic conditions, hydrogen atoms (H^+) in the solution could protonate to the amine group and thus cause an increase in pH [32].

Also, the highest dye sorption capacities were found to be at pH 6 and 8. If electrostatic interaction was the physical adsorption mechanism of the dye, in that case the capacity should be at a maximum within the range pH 6–8. In this pH range, the surface of polymer adsorbent is positively charged and dyes are negatively charged. The large increase in dye adsorption at basic conditions can be attributed to electrostatic pull between the positively charged polymer adsorbent and the deprotonated dye molecules. As a result, the adsorption capacity increased with increasing pH values.

Both natural sorbents and synthetic sorbents were prepared and used to remove dyes. Some important sorbents which used dye removal are given in Table 4. Dye sorption capacities of the sorbents are dependent on the sorbents structure and dyes types.

PVI-g-PVBC resin is core-shell type structure. PVBC has hydrophobic character whereas PVI is hydrophilic polymer. Therefore, core-shell structure gives semi-homogenous reaction medium for resin to remove dyes from water and gain hydrophilic character.

Table 2
Dye sorption capacity depending on the amount of the resin

Adsorbent amount (g)	Capacity (mg dye/g resin)
0.025	60
0.050	80
0.100	100
0.200	111
0.250	90

Table 3
Maximum dye sorption capacities of the PVI grafted PVBC resin depending on pH

Dye	pH	Capacity (mg dye/g resin)
Reactive Red	2.0	4.20
	4.0	4.60
	6.0	5.50
	8.0	4.10
Remazol Black	2.0	9.20
	4.0	9.00
	6.0	9.80
	8.0	8.90
Calcon	2.0	101
	8.0	116

3.3. Dye sorption kinetics of the resin

Batch kinetic sorption experiments were performed by using highly diluted dye solutions to investigate the efficiency of the resin in the presence of trace quantities of dyes.

The concentration–time plot (Fig. 7) shows that within about 40 min contact time, the dye concentration falls to zero.

Kinetics is important for adsorption studies because it can predict the rate at which a pollutant is removed from aqueous solutions and provides valuable data for understanding the mechanism of sorption reactions. In order to investigate the kinetic of dyes uptake process, pseudo-first-order and pseudo-second-order models have been examined (Table 5).

The Lagergren first-order rate equation is one of the most widely used equations for the sorption of solute from a liquid solution. A linear form of pseudo-first-order equation of Lagergren is generally expressed as:

Table 4
Some synthetic polymer adsorbents, target dyes and corresponding adsorption capacities

Various types of adsorbents	Dyes	Q_{max} (mg/g)	References
Quaternized sugarcane bagasse	Reactive orange 16	22.73	[33]
Polypyrrole-modified-a-cellulose	Reactive red 120	96.1	[34]
Composites of GO-MWCNT	Congo red	66.7	[35]
Chitosan-based hydrogel	Erichrome black T	520.21	[36]
Chitosan/graphene oxide nanocomposit	Acid yellow and acid blue (binary)	60.0	[37]
TiO_2/NiO coupled nanoparticles	Reactive red 46	102.1	[38]
Purolite C145 macroporous polymeric ion exchangers	Direct blue 9	31.98	[39]
Trapa bispinosa's fruit	C.I. Reactive orange 122	29.51	[40]
Semi-IPN cellulose-graft-polyacrylamide/hydroxyapatite biocomposite hydrogel	Reactive blue 2	173.6	[41]
Powdered activated carbon	Acid orange 7	34.52	[42]
ZnS nanoparticles-loaded activated carbon	Eosin B	100.19	[43]
HDTMA-bentonite	Reactive red 141	70–110	[44]
Semi-IPN superabsorbent chitosan-starch hydrogel	Direct Red 80	312.77	[45]
Polymer-clay composite [P (AAm-AA)-Kao]	Bromophenol blue	92.4	[46]
PPy/mw nanocomposite	Congo red	147.0	[47]
Partial diethylamino-ethylated cotton dust waste	C.I. Reactive red 239	86.96	[48]
L-Arginine-functionalized Fe_3O_4 nanoparticles	C.I. Reactive batch blue 19	66.66	[49]

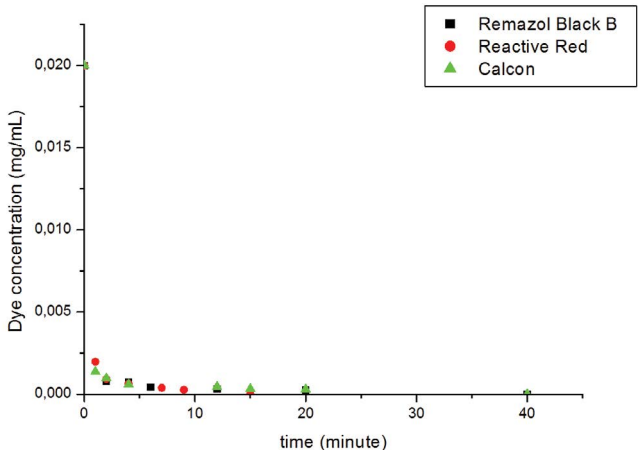

Fig. 7. Sorption kinetics of the resin.

$$\log\left(\frac{q_{eq}}{q_{eq}-q_t}\right)=\frac{(k_1\times t)}{2.303} \tag{13}$$

where q_e and q_t (both in mg/g) are the amount of dye adsorbed per unit mass of adsorbent at equilibrium and time t (min), respectively. The slopes and intercepts of plots of log ($q_{eq} - q_t$) vs. t were used to determine the pseudo-first-order rate constant k_1 and q_{eq}.

The kinetic data were treated with the following Ho and McKay [50] pseudo-second-order rate equation:

The linear form of the equation describing the adsorption kinetics by the pseudo-second-order model is as follows:

$$\frac{t}{q_t}=\frac{1}{k_2q_e^2}+\frac{1}{q_e}t \tag{14}$$

where q_e is the amount of dye adsorbed at equilibrium (mg g^{-1}); q_t is the amount of dye adsorbed at time t (mg g^{-1}); and k_2 is the equilibrium rate constant of pseudo-second-order sorption (g mg^{-1} min^{-1}).

The q_e and k_2 values could be calculated from the slopes ($1/q_e$) and intercepts ($1/k_2q_e^2$) of linear plots of t/q_t vs. t. The pseudo-second-order model plots of the dye sorption are shown in Fig. 8.

The pseudo-second-order model predicts the adsorption behavior over the whole range of adsorption period and it is in agreement with the chemisorption mechanism being the rate controlling step. Chemical sorption involves valence forces through sharing or exchange of electrons between adsorbent and adsorbate.

The high values of correlation coefficients showed that the data fitted well to the pseudo-second-order rate kinetic model (Table 5).

3.4. Regeneration of the resin

Loaded polymer samples, when treated with basic methanol become almost dye-free. In this way, 92% of dye was recovered 102 mg dye per g of loaded sample. Regeneration and reusability of the resin was performed and it is used for at least five cycles and desorption capacity of the resin was found to be 90 mg dye/g loaded sample.

4. Conclusions

In this work, PVI grafted onto PVBC resin was synthesized to prepare an alternative adsorbent for removal of acidic dyes from wastewater. ATRP polymerization of vinyl (imidazole) (VI) in the presence of only CuBr as catalyst is difficult. Therefore, graft copolymerization of PVI onto PVBC was carried out using reverse ATRP method. The sorption

Table 5
Pseudo-first-order and second-order kinetics models for adsorption of dyes on the resin

Dyes	First order			Second order		
	q_e	k_1	R^2	k_2	q_e	R^2
	(mg g^{-1})	(min^{-1})		(mg g^{-1} min^{-1})	(mg g^{-1})	
Reactive Red	2.77	0.29	0.730	0.95	19.72	0.999
Remazol Black	5.68	0.57	0.910	0.70	20.70	0.999
Calcon	3.90	0.41	0.730	0.99	19.76	0.999

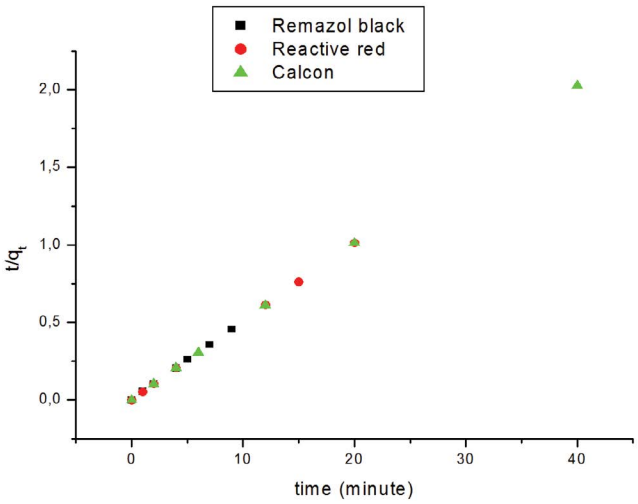

Fig. 8. Pseudo-second-order model plots of the dyes sorbed by the resin.

capacity of the flexibility of the side chains in the resin is expected to provide pseudo homogeneous reaction conditions and have the advantage of mobility of the graft chains in the removal of dyes from aqueous mixtures.

The results indicated that core-shell type polymeric resin demonstrates greater potential for acidic dyes removal from water.

Also, as a result of isotherm studies, it has been found that the adsorption of dyes on polymeric resin is best described by Langmuir isotherm. The maximum adsorption capacities (q_{max}) were calculated for Calcon, Reactive Red 195 and Remazol Black B, as 111, 9.70 and 4.11 mg g^{-1}, respectively.

The values of bonding free energy were calculated from D-R isotherm equation and these values found to be 261, 163 and 99 J mol^{-1} for Calcon, Reactive Red 195, Remazol Black B, respectively. Since the molecular structure of the Calcon dye is small and the molar mass is low, its sorption capacity is higher than the other dyes. Therefore, the bond free energy of Calcon is higher than other dyes. Also, the resin can be used for a wide pH range. As a result, the resin could be used wastewater treatment which contains acidic dyes.

Acknowledgment

This research has been supported by Scientific Research Project Coordination Center of Istanbul Technical University (project number: 37755).

References

[1] X.F. Sun, J.K. Liu, M.L. Lee, Surface modification of glycidyl-containing poly(methyl methacrylate) microchips using surface-initiated atom-transfer radical polymerization, Anal. Chem., 80 (2008) 856–863.
[2] B. Zhao, W.J. Brittain, Polymer brushes: surface-immobilized macromolecules, Prog. Polym. Sci., 25 (2000) 677–710.
[3] O. Prucker, J. Ruhe, Mechanism of radical chain polymerizations initiated by azo compounds covalently bound to the surface of spherical particles, Macromolecules, 31 (1998) 602–613.
[4] O. Prucker, J. Ruhe, Synthesis of poly(styrene) monolayers attached to high surface area silica gels through self-assembled monolayers of azo initiators, Macromolecules, 31 (1998) 592–601.
[5] O.H. Kwon, Y.C. Nho, J.H. Jin, M.J. Lee, Y.M. Lee, Graft polymerization of methyl methacrylate onto radiation-peroxidized ultrahigh molecular weight polyethylene in the presence of metallic salt and acid, J. Appl. Polym. Sci., 72 (1999) 659–666.
[6] M.K. Sreedhar, T.S. Anirudhan, Preparation of an adsorbent by graft polymerization of acrylamide onto coconut husk for mercury(II) removal from aqueous solution and chloralkali industry wastewater, J. Appl. Polym. Sci., 75 (2000) 1261–1269.
[7] X.K. Xu, A.M. Lenhoff, A predictive approach to correlating protein adsorption isotherms on ion-exchange media, J. Phys. Chem., B, 112 (2008) 1028–1040.
[8] P. Liu, J.S. Guo, Polyacrylamide grafted attapulgite (PAM-ATP) via surface-initiated atom transfer radical polymerization (SI-ATRP) for removal of Hg(II) ion and dyes, Colloids Surf., A, 282 (2006) 498–503.
[9] J. Pyun, T. Kowalewski, K. Matyjaszewski, Synthesis of polymer brushes using atom transfer radical polymerization, Macromol. Rapid Commun., 24 (2003) 1043–1059.
[10] K. Nagase, J. Kobayashi, A.I. Kikuchi, Y. Akiyama, H. Kanazawa, T. Okano, Effects of graft densities and chain lengths on separation of bioactive compounds by nanolayered thermoresponsive polymer brush surfaces, Langmuir, 24 (2008) 511–517.
[11] T.Q. Liu, S.J. Jia, T. Kowalewski, K. Matyjaszewski, R. Casado-Portilla, J. Belmont, Water-dispersible carbon black nanocomposites prepared by surface-initiated atom transfer radical polymerization in protic media, Macromolecules, 39 (2006) 548–556.
[12] F.J. Xu, Q.J. Cai, Y.L. Li, E.T. Kang, K.G. Neoh, Covalent immobilization of glucose oxidase on well-defined poly(glycidyl methacrylate)–Si(111) hybrids from surface-initiated atom-transfer radical polymerization, Biomacromolecules, 6 (2005) 1012–1020.
[13] J.A. Seo, Y.W. Kim, D.K. Roh, Y.G. Shul, J.H. Kim, Proton conducting grafted/crosslinked membranes prepared from poly(vinylidene fluoride-co-chlorotrifluoroethylene) copolymer, Polym. Adv. Technol., 22 (2011) 1434–1441.
[14] M. Zhang, T.P. Russell, Graft copolymers from poly(vinylidene fluoride-co-chlorotrifluoroethylene) via atom transfer radical polymerization, Macromolecules, 39 (2006) 3531–3539.
[15] H. Bottcher, M.L. Hallensleben, S. Nuss, H. Wurm, ATRP grafting from silica surface to create first and second generation of grafts, Polymer Bull., 44 (2000) 223–229.

[16] K.L. Beers, S.G. Gaynor, K. Matyjaszewski, The use of ''living'' radical polymerization to synthesize graft copolymers, Abstr. Papers Am. Chem. Soc., 211 (1996) 86.
[17] N. Bicak, B.F. Senkal, Aldehyde separation by polymer-supported oligo(ethyleneimines), J. Polym. Sci. Part A – Polym. Chem., 35 (1997) 2857–2864.
[18] B.F. Senkal, N. Bicak, Grafting on crosslinked polymer beads by ATRP from polymer supported N-chlorosulfonamides, Eur. Polym. J., 39 (2003) 327–331.
[19] H.B. Sonmez, B.F. Senkal, D.C. Sherrington, N. Bicak, Atom transfer radical graft polymerization of acrylamide from N-chlorosulfonamidated polystyrene resin, and use of the resin in selective mercury removal, React. Funct. Polym., 55 (2003) 1–8.
[20] B.F. Senkal, E. Yavuz, Preparation of poly(vinyl pyrrolidone) grafted sulfonamide based polystyrene resin and its use for the removal of dye from water, Polym. Adv. Technol., 17 (2003) 928–931.
[21] B. Yu, F. Zhou, H. Hu, C.W. Wang, W.M. Liu, Synthesis and properties of polymer brushes bearing ionic liquid moieties, Electrochim Acta, 53 (2007) 487–494.
[22] M.K. Samantaray, V. Katiyar, K.L. Pang, H. Nanavati, P. Ghosh, Silver N-heterocyclic carbene complexes as initiators for bulk ring-opening polymerization (ROP) of l-lactides, J. Organomet. Chem., 692 (2007) 1672–1682.
[23] N. Le Poul, M. Campion, B. Douziech, Y. Rondelez, L. Le Clainche, O. Reinaud, Y. Le Mest, Monocopper center embedded in a biomimetic cavity: from supramolecular control of copper coordination to redox regulation, J. Am. Chem. Soc., 129 (2007) 8801–8810.
[24] V.J. Catalano, A.O. Etogo, Preparation of Au(I), Ag(I), and Pd(II) N-heterocyclic carbene complexes utilizing a methylpyridyl-substituted NHC ligand. Formation of a luminescent coordination polymer, Inorg. Chem., 46 (2007) 5608–5615.
[25] N. Preethi, H. Shinohara, H. Nishide, Reversible oxygen-binding and facilitated oxygen transport in membranes of poly-vinylimidazole complexed with cobalt-phthalocyanine, React. Funct. Polym., 66 (2006) 851–855.
[26] M.G. Organ, S. Avola, I. Dubovyk, N. Hadei, E.A.B. Kantchev, C.J. O'Brien, C. Valente, A user-friendly, all-purpose Pd–NHC (NHC= N-heterocyclic carbene) precatalyst for the Negishi reaction: a step towards a universal cross-coupling catalyst, Chem. Eur. J., 12 (2006) 4749–4755.
[27] E.B. Anderson, T.E. Long, Imidazole-and imidazolium-containing polymers for biology and material science applications, Polymer, 51 (2010) 2447–2454.
[28] E. Yavuz, G. Bayramoglu, M.Y. Arica, B.F. Senkal, Preparation of poly (acrylic acid) containing core-shell type resin for removal of basic dyes, J. Chem. Technol. Biotechnol., 86 (2011) 699–705.
[29] Y.C. Wong, Y.S. Szeto, W.H. Cheung, G. McKay, Adsorption of acid dyes on chitosan—equilibrium isotherm analyses, Process Biochem., 39 (2004) 693–702.
[30] I. Szaraz, W. Forsling, A spectroscopic study of the solvation of 1-vinyl-2-pyrrolidone and poly (1-vinyl-2-pyrrolidone) in different solvents, Polymer, 41 (2000) 4831–4839.
[31] M. Horsfall, A.I. Spiff, Equilibrium sorption study of Al^{3+}, Co^{2+} and Ag^{+} in aqueous solutions by fluted pumpkin (*Telfairia occidentalis* HOOK f) waste biomass, Acta Chim. Slov., 52 (2005) 174–181.
[32] M.S Chiou, P.Y. Ho, H.Y. Li, Adsorption of anionic dyes in acid solutions using chemically cross-linked chitosan beads, Dyes Pigm., 60 (2004) 69–84.
[33] S.Y Wong, Y.P Tan, A.H. Abdullah, S.T. Ong, The removal of basic and reactive dyes using quaternized sugarcane bagasse, J. Phys. Sci., 20 (2009) 59–74.
[34] V.M. Ovando-Medina, J. Vizcaíno-Mercado, O. Gonz alez-Ortega, J.A.R. De La Garza, H. Martínez-Guti errez, Synthesis of a-cellulose/polypyrrole composite for the removal of reactive red dye from aqueous solution: kinetics and equilibrium modeling, Polym. Compos., 36 (2015) 312–321.
[35] M.O. Ansari, R. Kumar, S.A. Ansari, S.P. Ansari, M.A. Barakat, A. Alshahrie, M.H. Cho, Anion selective pTSA doped polyaniline@graphene oxidemultiwalled carbon nanotube composite for Cr(VI) and Congo red adsorption, J. Colloid Interface Sci., 496 (2017) 407–415.
[36] A.A. Oladipo, M. Gazi, E. Yilmaz, Single and binary adsorption of azo and anthraquinone dyes by chitosan-based hydrogel: selectivity factor and Box-Behnken process, Chem. Eng. Res. Design, 104 (2015) 264–279.
[37] P. Banerjee, S.R. Barman, A. Mukhopadhayay, P. Das, Ultrasound assisted mixed azo dye adsorption by chitosan–graphene oxide nanocomposite, Chem. Eng. Res. Des., 117 (2017) 43–56.
[38] H. Eskandarloo, A. Badiei, C. Haug, Enhanced photocatalytic degradation of an azo textile dye by using TiO_2/NiO coupled nanoparticles: optimization of synthesis and operational key factors, Mater. Sci. Semicond. Process., 27 (2014) 240–253.
[39] S. Daniela, B. Doina, C. Sergiu, Macroporous polymeric ion exchangers as adsorbents for the removal of cationic dye basic Blue 9 from aqueous solutions, J. Appl. Polym. Sci., 131 (2014) 39620 (1–12).
[40] M. Saeed, R. Nadeem, M. Yousaf, Removal of industrial pollutant (Reactive Orange 122 dye) using environment-friendly sorbent *Trapa bispinosa*'s peel and fruit, Int. J. Environ. Sci. Technol., 12 (2015) 1223–1234.
[41] A.A. Oladipo, M. Gazi, S.S. Samandari, Adsorption of anthraquinone dye onto eco-friendly semi-IPN biocomposite hydrogel: equilibrium isotherms, kinetic studies and optimization, J. Taiwan Inst. Chem. Eng., 45 (2014) 653–664.
[42] S. Aber, N. Daneshvar, S.M. Soroureddin, A. Chabok, K. Asadpour-Zeynali, Study of acid orange 7 removal from aqueous solutions by powdered activated carbon and modeling of experimental results by artificial neural network, Desalination, 211 (2007) 87–95.
[43] M. Jamshidi, M. Ghaedi, K. Dashtian, A.M. Ghaedi, S. Hajati, A. Goudarzi, E. Alipanahpour, Highly efficient simultaneous ultrasonic assisted adsorption of brilliant green and eosin B onto ZnS nanoparticles loaded activated carbon: artificial neural network modeling and central composite design optimization, Spectrochim. Acta A, 153 (2016) 257–267.
[44] S. Elemen, E.P.A. Kumbasar, S. Yapar, Modeling the adsorption of textile dye on organoclay using an artificial neural network, Dyes Pigm., 95 (2012) 102–111.
[45] F.A. Ngwabebhoh, M. Gazi, A.A. Oladipo, Adsorptive removal of multi-azo dye from aqueous phase using a semi-IPN super-absorbent chitosan-starch hydrogel, Chem. Eng. Res. Design, 112 (2016) 274–288.
[46] A.A. El-Zahhar, N.S. Awwad, E.E. El-Katori, Removal of bromophenol blue dye from industrial waste water by synthesizing polymer-clay composite, J. Mol. Liq., 199 (2014) 454–461.
[47] R.S. Aliabadi, N.O. Mahmoodi, Synthesis and characterization of polypyrrole, polyaniline nanoparticles and their nanocomposite for removal of azo dyes; sunset yellow and Congo red, J. Cleaner Prod., 179 (2018) 235–245.
[48] J.D. Fontana, G.R. Baldo, A. Grzybowski, M. Tiboni, L. Blitzkow Scremin, H. Koop, M.J. Santana, L.M. Lião, J.D. Fontana, Textile cotton dust waste: partial diethylamino-ethylation and its application to the sorption/removal of the model residual textile dye Reactive Red, Polym. Bull., 73 (2016) 3401–3420.
[49] A. Dalvand, R. Nabizadeh, M. Reza Ganjali, M. Khoobi, S. Nazmara, A. Hossein Mahvi, Modeling of Reactive Blue 19 azo dye removal from colored textile wastewater using L-arginine-functionalized Fe_3O_4 nanoparticles: optimization, reusability, kinetic and equilibrium studies, J. Magn. Magn Mater., 404 (2016) 179–189.
[50] Y.S. Ho, G. McKay, Pseudo-second order model for sorption processes, Process Biochem., 34 (1999) 451–465.